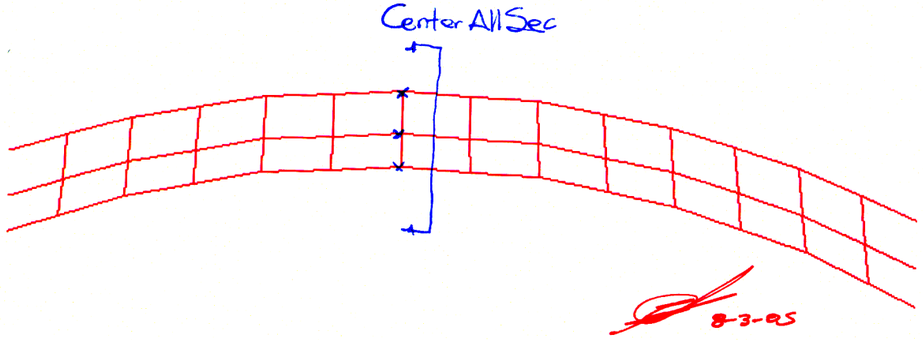

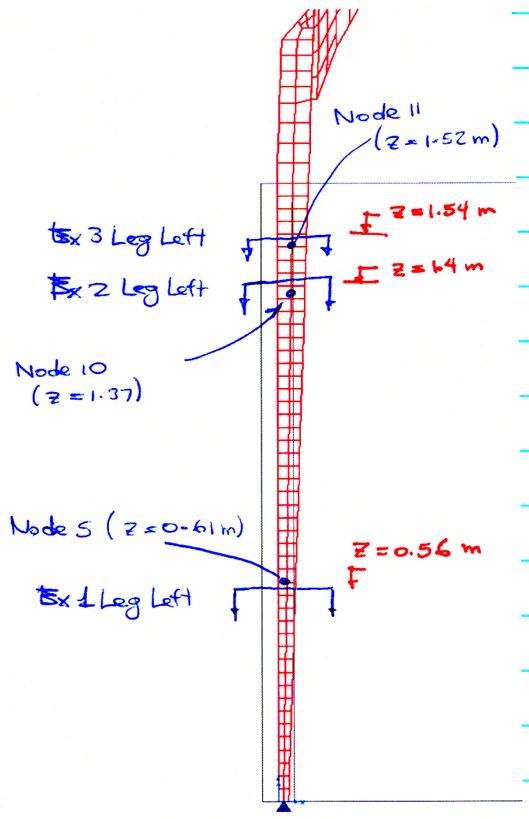

Note that the section cut Ex 6 Left Corn is not a straight line (the initial modeling was not developed with this cut in mind) and should be taken only as an approximation. Other section cuts that have the same ~~edges~~ end points of Ex 6 Left Corn LE 8-3-05 will have different end forces.

The first ~~static~~ loading case analyzed is a system LE 8-3-05 ~~symmetry~~ with overpressure applied locally to the crown. This case is not a realistic loading configuration but for comparison purposes presents valuable information.

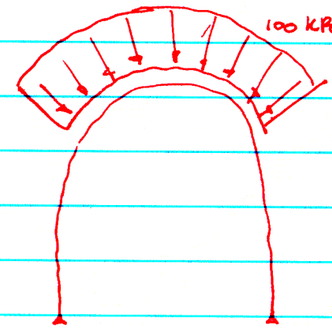

(See Case 3 in page 38)

Based on the above load distribution x have been obtained the bending moments of different locations using SAP2000 Frame model and SAP2000 ~~FEM~~. The bending moment diagram from FEM, LE 8-3-05 from the frame model and the section cut forces are presented in next page

BENDING MOMENT DIAGRAM (KN-m)

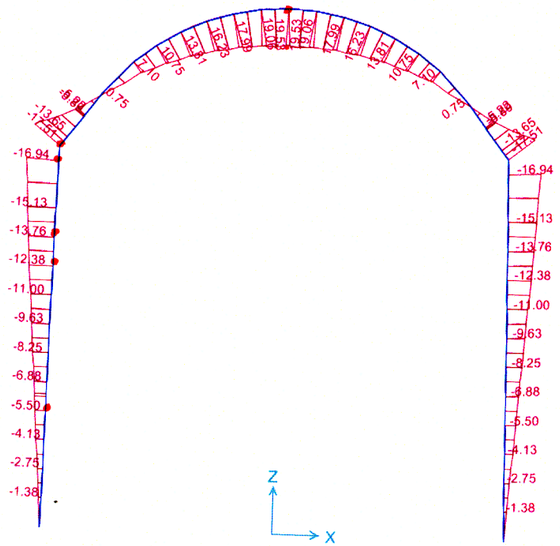

8-3-05

Table: Section Cut Forces, Part 1 of 3

SectionCut Text	OutputCase Text	F1 KN	F3 KN	Moment FEM KN-m	Moment Frame, KN-m
CenterAllsec	OverpLoc	-82.215	-7.662E-10	-23.1277	19.53
Ex1CornLeft	OverpLoc	-13.271	-122.359	16.8183	-16.94
Ex6CornLeft	OverpLoc	14.087	121.737	-14.7877	-17.51
Ex1LegLeft	OverpLoc	-13.271	-122.359	4.1261	-5.50
Ex2LegLeft	OverpLoc	-13.271	-122.359	12.1639	-12.38
Ex3LegLeft	OverpLoc	-13.271	-122.359	13.5035	-13.76

8-3-05

As observed, the moments at comparable locations are in good agreement. Note that some of the moments from the FEM have opposite signs with respect to those generated

by the frame model, due to the way in which the section cuts were defined in FEM.
It must be kept in mind that DS-rubble interaction was not modeled in the SAP2000 FEM; therefore, the DS frame model did not include rubble springs. This is evident in the next loading configuration examined, in which concentrated loads of 100 KN were applied to the DS corners. Very large elastic moments were generated (it LI 8-03-05 assumed non-linear performance was not included) due to the large displacements that result from the elastic loading. (see case 2 in page 35).

Results for both model using the above loading configuration are shown below:

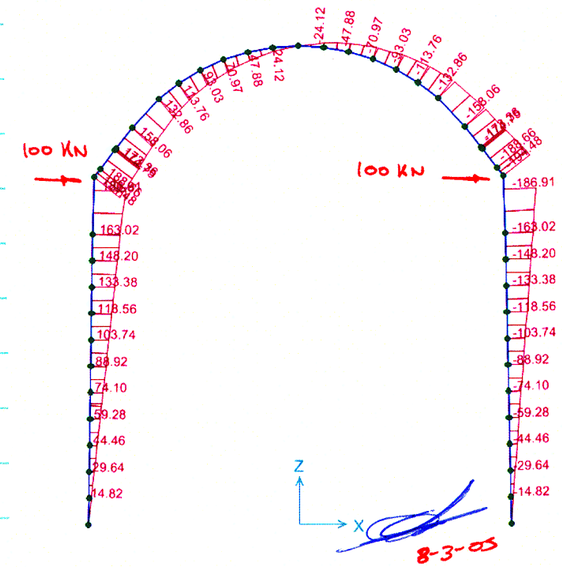

8-3-05

BENDING MOMENT DIAGRAM FOR FRAME MODEL (KN-m)

The moments at selected critical locations of the FEM are presented below, as well as bending moments from the frame model that are close to these critical locations. Good agreement is found for all cases.

Table: Section Cut Forces, Part 1 of 3

8-3-05

SectionCut Text	OutputCase Text	F1 KN	F3 KN	Moment FEM KN-m	Moment Frame, KN-m
CenterAllsec	HorPunc	7.622E-07	164.475	1.617E-04	0
Ex1CornLeft	HorPunc	100.000	164.475	-178.4603	186.91
Ex6CornLeft	HorPunc	1.502	-174.615	184.0741	194.48
Ex1LegLeft	HorPunc	100.000	164.475	-51.5020	59.28
Ex2LegLeft	HorPunc	100.000	164.475	-131.2400	133.38
Ex3LegLeft	HorPunc	100.000	164.475	-144.5297	148.20

A final example is presented for the following symmetric loading configuration:

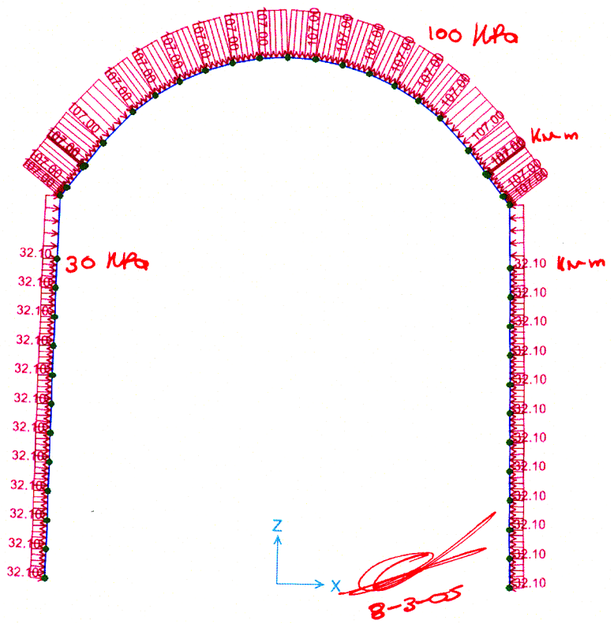

8-3-05

The bending moments for both cases are the following:

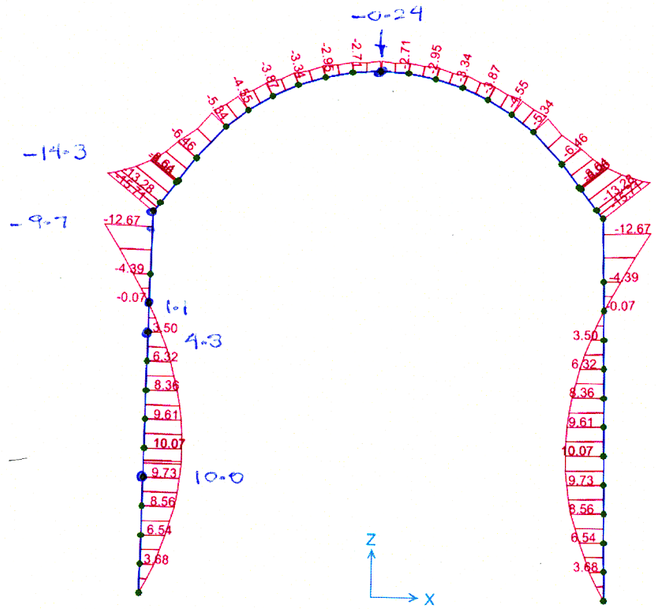

Table: Section Cut Forces, Part 1 of 3

SectionCut Text	OutputCase Text	F1 KN	F3 KN	Moment FEM KN-m	Moment Frame, KN-m
CenterAllsec	BaseSym	-117.717	1.463E-10	0.2376	-2.71
Ex1CornLeft	BaseSym	-40.110	-122.663	9.7291	-12.67
Ex6CornLeft	BaseSym	46.685	120.570	-14.2915	-15.71
Ex1LegLeft	BaseSym	2.917	-124.164	-10.0224	9.73
Ex2LegLeft	BaseSym	-24.065	-123.222	-4.2887	3.5
Ex3LegLeft	BaseSym	-28.562	-123.064	-1.1302	-.07

As observed, bending moments also present good agreement when the DS columns include an inflexion point. Therefore, these results indicate that the selected section properties for the DS frame, particularly the equivalent width, b_E, are adequate.

8-03-05

8-05-05

PIN CONSTRAINT AT DS BASE

The calculation of the DS strength capacity using the frame model assumes a pin constrain at the DS base. This constraint is a valid approximation if the frictional force developed between the DS and the invert surface is larger than the horizontal reaction at the DS base.

To validate the above assumption, the FEM developed in ABAQUS was analyzed for a prescribed loading configuration using two boundary conditions for the model: (a) a friction BC, and (b) a pin BC.

The FEM used for the analyses is shown below:

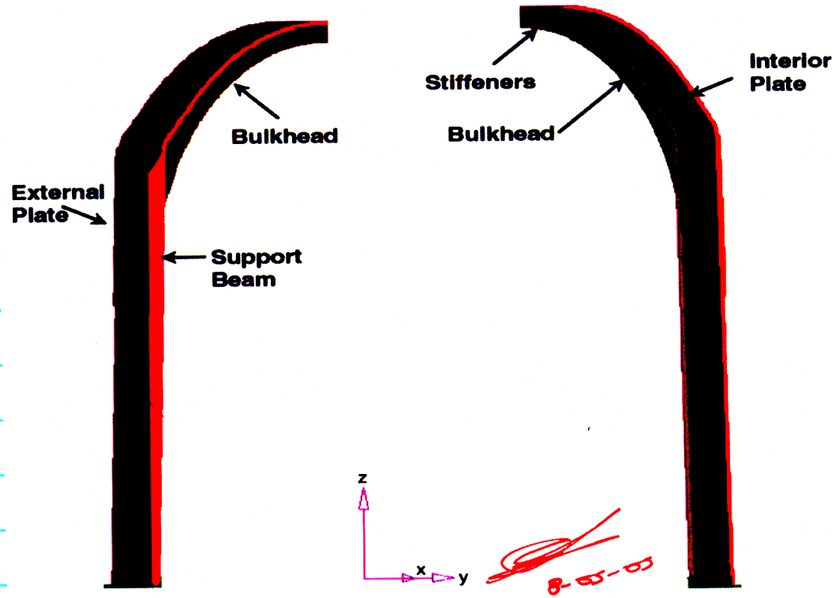

For the case of the friction support, a friction coefficient $\mu = 0.4$ was used. The loading configuration included a ratio of horizontal to vertical pressures of $P_h/P_v = 0.3$ (see figure below).

These proportional loads were applied as a linear ramp of pressure versus time.

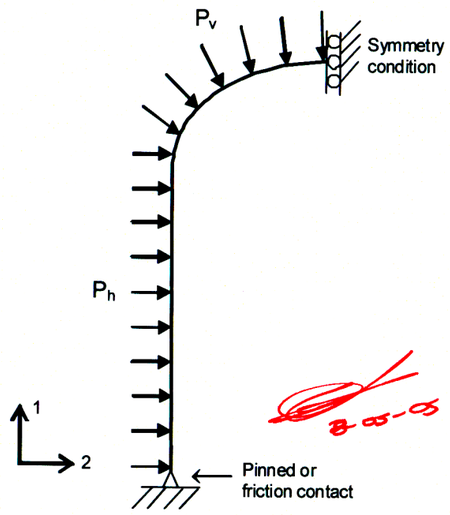

Both material and geometric nonlinearities were considered.

The results were expressed as a function of the maximum vertical pressure (in MPa) that can be applied to the DS before structural instability. LIF 8-05-05

In the figure of page 50, the results of vertical load carrying capacity are plotted versus the displacement measured at node 17990, which is located at the side of the DS at approximately 0.80m from the invert surface. (files: DSTiedpressure2d.inp for friction support model, and DStiedpressure3d.inp for the pin support model).

As observed, the structural response is very similar for both models, as long as the frictional force overcomes the DS base horizontal reaction.

DS Vertical Load Carrying Capacity vs Displacement at DS column (0.8 m from base)

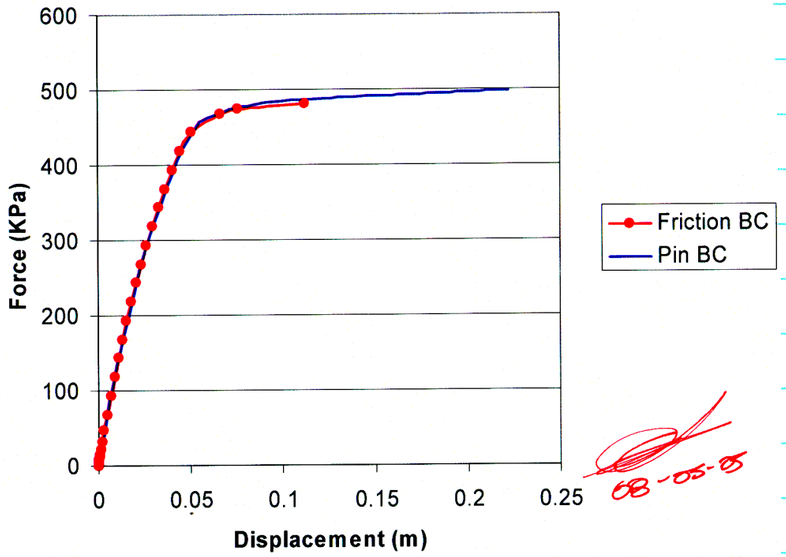

08-05-05

DRIP SHIELD - WASTE PACKAGE MECHANICAL INTERACTION

Feb 15,06

The drip shield - waste package (DS-WP) interaction needs to be evaluated because the updated DS design cannot withstand the expected loading conditions, according to the structural analyses in SAP 2000 & ABAQUS.

WP (LI, Feb 15,06)

One of the main considerations is the definition of "failure mode", which was defined for the first stage of the analyses as follows:

Luis Ibarra

From: Luis Ibarra [libarra@cnwra.swri.edu]
Sent: Friday, December 16, 2005 5:21 PM
To: 'Aladar Csontos'
Cc: 'Thomas Wilt'
Subject: RE: Mechanical Failure Criteria Meeting 12-19-05 2-4:30pm (EST)

Failure Mode Definition Dec 16...

Al,

This is what part of what we want to discuss next Monday.

Have a good weekend.

Luis

File: Failure Mode Definition Dec 16. doc

Not predecisional anymore 10/17/07

~~PREDECISIONAL - INTERNAL USE ONLY~~ Feb 15,06

Mechanical Interaction of Drip Shield and Waste Package Failure Mode

The drip shield (DS) -waste package (WP) interaction is caused by potential DS structural failure. A collapsed DS would transfer permanent static loads to the WP outer shell, loads that may be amplified due to seismic ground motions. On the other hand, the mechanical properties of the outer shell are affected by high temperatures, and the potential for generalized corrosion for very long periods of time.

The breaching of the waste package outer barrier is physically associated with cracks that propagate throughout the plate depth. Assuming that stress corrosion cracking is highly unlikely, it is plausible to consider that in a compressive strain field, cracks of enough size to permit the intrusion of water will occur only when the strains are close to the rupture strain of the material. Analyses involving ultimate strain, however, require complex finite element analyses. For instance, so-called post-peak material behavior require continuum damage models because rupture strain of ductile materials such as Alloy-22, takes place after the ultimate tensile strength (UTS) has been reached. That is, after the plateau of the engineering stress-strain curve, there is a softening of the material characterized by a negative slope, which indicates that necking of the material has initiated.

The NRC/Center staff is following a step-by-step approach to investigate the potential breaching of the WP outer barrier. The analyses include static and dynamic loading, and each new step involves more complex geometry of the finite element models (FEMs), and more sophisticated definitions of analytical failure modes, which are closer to the physical definition of failure mode. Another reason for this approach is the need to provide reasonable information to the performance assessment group by the end of January, 2006. The potential definition of failure mode for the analytical models are summarized below.

WP failure criterion to be used in the current TPA abstraction

Alloy-22 is a very ductile material that has a minimum elongation of 0.45, according to the ASME code. The limited available engineering stress-strain curves for Alloy-22 indicate that the strain when the ultimate tensile strength (UTS) occurs is approximately 80-90% of the ultimate strain. After the UTS point, the material presents necking and softening of the engineering stress-strain curve. At this stage, a system with no redundancy is structurally unstable under static monotonic loads. In the case of the waste package outer shell, the system should be able to redistribute some of the stresses and increase its loading capacity. This increase in capacity is expected to be marginal because the material has already increased significantly its resistance in the nonlinear range, and because the strain at the UTS is close to the ultimate strain.

Therefore, the FEMs of this first stage consider the reaching of the UTS as the analytical failure mode. These FEMs utilize non-deteriorating models that cannot reproduce the structural performance after the UTS point has been surpassed,. The approach is conservative not only because considers failure based on the UTS, but also because failure is assumed as soon as the

Not predecisional anymore 10/17/07

~~PREDECISIONAL - INTERNAL USE ONLY~~ Feb 15,06

first Alloy-22 element reaches this value. Evidently, the first elements reaching this stress level are located in the area surrounding the contact region. At first glance, it appears that conservatism may be reduced by considering failure when a substantial region of the Alloy-22 plate has reached the UTS. This option, however, is not viable because non-deteriorating models significantly overestimate the capacity of all the elements that at early loading stages reach the UTS and should exhibit material softening.

These conservative analyses consider thermal effects by using material properties degraded by the presence of expected high temperatures. Also, quasi-static loads are initially used to represent the dynamic loads expected during seismic events. Preliminary results indicate that there is a large safety margin against breaching of the WP outer barrier due to static loads, even when the above conservative definition of failure mode is used.

Long-term work plan on the development of failure mode criterion

More sophisticated finite element analysis techniques would be required if the above conservative assumptions predict failure at early loading stages. In this case, several options are available.

I. Appropriate continuum damage mechanics model. The model should be capable of accounting for the softening/damage region of the of the engineering stress-strain curve. The "crack" in the material would be represented by the resulting bands of damaged elements which have no stiffness associated with them. Mesh dependence (characteristic lengths of the elements) of the solutions will need to be addressed. Because of the high temperature of the waste package, possible creep crack growth effects may also need to be investigated. This type of crack growth would require the use of a time-dependent material model in conjunction with the continuum damage approach.

II. Fracture mechanics analysis. These FEMs would use a two-surface, double node in the zone in which the crack is assumed to occur. In this approach, a zone containing master and slave surfaces are created which are initially in contact (i.e. bonded together). The propagation of the crack through the material would be simulated using a "debonding" criterion, which may use normal and shear components.

Feb 15,06

March 03, 06

Based on the failure mode defined in pages 52 & 53, finite element analyses (FEA) were performed in ABAQUS. The detailed description and presentation of results is in SN #764 for plane strain models. This notebook is mainly used by Dr. Thomas Wilt. The results for 3-D models are documented in SN 772E, which is mainly maintained by Dr. Roman Kozlan.

The summary of the above analyses, as well as the description of the DS-WP interaction and the resulting MECHFAIL abstractions, were documented in a draft sent to NRC staff on January 31, 06. Also, an internal presentation of the draft was performed on March 02, 06 to NRC & CNWRA Performance Assessment staff.

The following pages show material that was used in the preparation of the draft and the presentation.

DS-WP MECHANICAL INTERACTION

If the DS collapses, the WP outer shell (OS) has to withstand permanent static loads that may be amplified due to seismic ground motions. For the DS-WP interaction analyses, additional uncertainty is found with respect to traditional analyses because the DS deformed shape is unknown.

Collapsed DS and DS-WP Mechanical Interaction

03-03-06

Several studies (MECHFAIL, DS report) indicate that DS collapse would be triggered by plastic buckling of the DS "support beams" (columns). There are, however, a large number of scenarios that may lead to DS collapse, including different static loading configurations, seismic events of different characteristics, temperature variations, invert degradation, creep, etc. All of these variables result in large uncertainty regarding the final shape of the collapsed DS. Nevertheless, there are some conditions that need to be present in order to cause WP failure. For instance, stress concentration on the WP OS is relevant only if the DS edge impacts the WP with a certain angle because the contact area between the components is reduced. A reduction in the contact area increases the potential for penetration of the DS component into the WP, or crack propagation in the WP OS. The angle between the DS edge and the tangent to the WP OS is called the "contact angle" in this study.

For the structural DS-WP evaluation, several assumptions were adopted for the initial configuration of the interaction based on the current design of the DS and the WP:

* The DS components having sharp edges that may cause large mechanical stresses in the WP are the bottom flange of the bulkhead and the longitudinal stiffeners, both of which are located in the DS crown (**Figure 1**). The support beams are welded on the external side of the DS walls made of Ti-7 plate. Therefore, the potential mechanical interaction at the sides is neglected because the DS component is the Ti-7 plate, resulting in mechanical stresses that are relatively low due to the absence of DS sharp edges.

* If the crown is not seriously damaged previous to complete DS collapse, the DS components that are expected to have the initial contact with the WP are the bulkheads. The longitudinal axis of the bulkheads is perpendicular to the longitudinal direction of the waste packages. Thus, if the DS crown were simply lowered, the entire bottom flange width would be in contact with the WP OS, but even under these circumstances, the initial contact area would be very limited because the radius of the WP is smaller than that of the DS crown. Nevertheless, as the permanent static loading were transferred from the DS crown to the WP, the bulkhead deformations would increase, leading to a larger contact area as the DS wrapped around the WP OS. This scenario in which the contact angle is close to zero is not expected to result in WP large mechanical stresses.

* Because of the initial geometry of the DS and the WP, contact angles between the bulkhead and the OS larger than zero may be triggered by local twisting of the bulkhead, by partial collapse of the DS, or by tilting of the WP. For the updated DS design, any of these alternatives lead to small contact angles in a significant percentage of the cases.

i) Local twisting of the bulkhead is expected to decrease significantly in the updated DS design because of the three longitudinal stiffeners that will prevent the rotation of the bulkhead (**Figure 1**).

ii) Partial collapse of the DS may cause large contact angles between DS bulkhead and the WP OS. However, partial collapse of the DS will occur for isolated DS sections, or at the end of a series of collapsed DS sections. Therefore, although the contact angle may be large for this situation, the percentage of DS's exhibiting local collapse is expected to be low.

iii) WP settlement or tilting in the longitudinal direction may lead to bulkhead contact angles larger than zero, even if the DS collapses uniformly and there is no twisting of the bulkhead. The WPs rest on pallets mantaining an initial horizontal position. The WP, however, may lose its horizontal position due to several reasons:

- Differential settlements. These settlements may occur when the grid of carbon-steel beams of the invert degrades. Then, the tuff material of the invert would have to carry the weight of the WP and be subjected to differential settlements. The properties of the tuff material have not been defined, and no precise calculation of the bearing capacity or differential settlement exists. Although the tuff material may behave satisfactorily under loads that only include the WP weight, if the invert degrades faster at one WP end, the likelihood of differential settlements will be high.

03-03-06

- The pallet includes four longitudinal components made of square tubular sections that provide rigidity in the longitudinal direction. These elements are made of 316 SS

(stainless steel) and because of long-term corrosion, these elements should be significantly degraded by the time the DS collapses. If no credit is taken for these elements, the pallet is highly susceptible to structural instability. In this case, one of the two supports, or both, may fail, which would cause tilting of the WP. Even under this scenario, the contact angle between the DS and the WP OS would be very likely less than 10 degrees.

* Mechanical interaction between longitudinal stiffeners and WP OS. If the DS collapse is relatively uniform, the longitudinal stiffeners do not have immediate contact with the WP OS because the stiffeners rest on top of the bulkhead bottom flange (**Figure 1**). Therefore, the stiffeners have to bend approximately 20 mm (in a span of 1047 mm) to contact the WP OS. This level of stiffener deformation requires loads larger than those expected to be transferred by the DS. However, if these flexural deformations occurred, the contact angle for most of the DS collapse cases would be between 0 and 10 degrees for the most critical of the three longitudinal stiffeners. Also, the tributary area for the longitudinal stiffeners is about 4-5 times smaller than that of the bulkhead components. Thus, the mechanical interaction with longitudinal stiffeners is not expected to be critical.

03-03-06

* Mechanical interaction between DS Ti-7 plates and WP OS. At the initial stages of mechanical interaction, contact between Ti-7 plates and the WP only takes place at the DS wall regions, where the Ti-24 components are welded at the external face of the shell. At later stages, the increase in static loads, seismic loads, or creep, may lead to interaction between the Ti-7 plates at the crown and the OS. These phenomenon would lead to a redistribution of stresses, relieving some of the loads transferred by the bulkhead to the WP OS.

* A collapsed DS still may be able to transfer loads to the invert throughout the damaged DS walls and support beams (columns). Even though the failure mechanism is plastic buckling of the DS walls, these components will be restrained by the pallet and WP. Nevertheless, a conservative assumption is made, and it is considered that all the vertical loads acting on top of the collapsed DS are transferred to the WP OS.

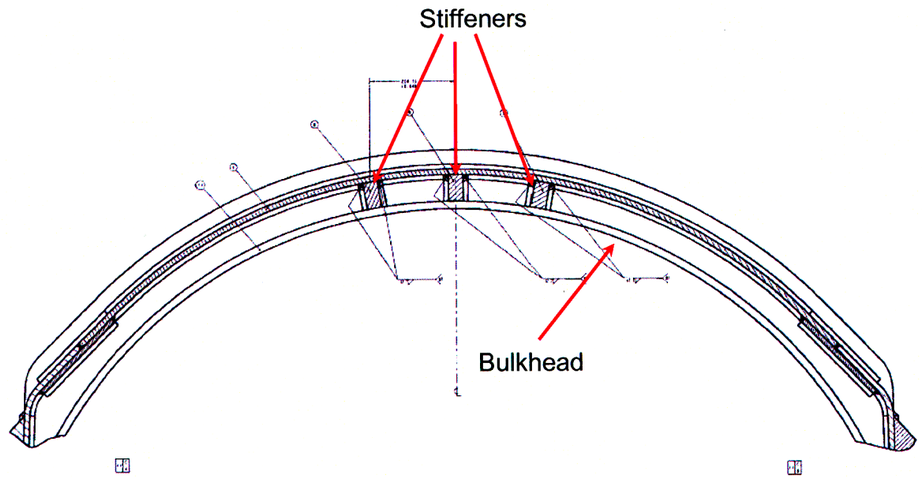

03-03-06

Figure 1

Plane Strain Finite Element Model

03-03-06

Description

FEMs of simple geometry were used to reproduce with large accuracy the mechanical interaction of the DS edges and the WP OS. The plane strain model is used to take advantage of the fact that the longitudinal direction is orders of magnitude larger than the displacement field generated in the transverse direction of the interaction. Also, it is desirable to minimize the model complexity because the initial contact between the DS edges and the WP OS produces a very small contact area, which demands a very fine mesh to accurately capture the localized stress and strain gradients. Therefore, a plane strain model that reduces the model to two dimensions was preferred to refine sufficiently the mesh without increasing significantly the time for the computational analysis.

Geometry

The curvature of the WP OS is not included in this model. This is a reasonable approximation because the displacement field due to mechanical interaction is very localized.

The WP OS and inner shell are assumed to be in contact, and the inner shell is represented as a rigid body. This simplification is justified because the outer shell is about 15 times more flexible than the inner shell.

To prevent penetration of the DS surface into the WP component, two measures were adopted. First, the edge of the DS components is rounded by introducing a radius R = 0.25 mm. This assures a small contact width between the two components when the first contact occurs. If a sharp edge were used instead, the initial contact width would be zero, and only deformation of the DS component edges will lead to a finite contact width.

The second measure to accurately model the stress and strain distribution is the adoption of a refined mesh. The contact elements of the DS are modeled as plane strain elements of 0.07x0.07 mm, whereas the contact elements of the WP OS plate are 0.13x0.18 mm shell elements.

Boundary Conditions

Loads. For most of the analyses, the DS component is loaded by a vertical body force located at the centroid. There are some analyses that include a tangential force to reproduce loading scenarios in which the load is not applied perpendicular to the tangent of the WP OS, and the vertical force is decomposed in a vertical and a horizontal load.

Kinematic Constraints. The plate simulating the WP OS is constrained from moving in the horizontal direction (1-axis), and the bottom surface is constrained from moving in vertical direction (2-axis) (See **Figures 2c and 2d)**. The last constrain simulates the rigid surface assumed for the inner vessel. The component representing the stiffener has roller supports at the diagonally opposite corners which allows only vertical translation of the stiffener. Also, two springs with a very small stiffness are used to prevent rigid body translation in the vertical direction.

The material properties used are those of Alloy-22 for the waste package outer vessel and Ti-24 for the stiffener. The specific values of these materials are given in the following table.

Table A. Material Properties of Alloy-22 and Ti-24

Material Property	Alloy-22	Ti-24
Elastic Modulus	197200 MPa	107200 MPa
Poisson's Ratio	0.31	0.31
True Yield Stress	254.7 MPa	658.1 MPa
Ultimate Tensile Strength:		
True Stress	954.1 MPa	804.4 MPa
True Strain	0.335	0.061

03-03-06

Three-Dimensional FEM

Three-dimensional FEMs were developed to verify some of the assumptions adopted in the plane strain models, or to provide data that cannot be obtained from the 2-D models. One of the main outcomes from the 3-D models is an estimate of the contact length of the bulkhead, as the DS wraps around the WP OS. Also, these models should provide insight into the overall performance after the WP OS deforms enough to contact the inner vessel. It is expected that the displacement history of the WP OS after the two plates make contact would be useful to validate the assumption of a rigid inner vessel used in the plane strain model. **Figure 3a** presents an isometric view of the 3-D model that is being currently developed.

The accuracy reached in the plane strain models cannot be obtained in the 3-D models. The main obstacle is that a similar degree of refinement for the solid elements of the 3-D model would result in a model with several million of elements.

Description

The finite element model is composed of the (i) the drip shield crown, (ii) the WP, and (iii) the emplacement pallet. The DS includes the Titanium Grade 24 bulkhead web and bottom flange, the Titanium Grade 24 longitudinal stiffeners, and the Titanium Grade 7 shell plate. The WP is represented by the Alloy 22 OS, and the 316 stainless steel inner shell. The emplacement pallet is represented by the Alloy 22 pallet plates (**Figure 3a**).

Geometry

The finite element model is constructed using the mixture of plate and solid elements. The following components are discretized 8-node continuum elements: bulkhead web, bulkhead flange; longitudinal stiffeners, WP OS, and inner shell. Also, a small number of 8-node linear

tetrahedral elements are used in the bulkhead. The shell plate and the pallet plates are made of quadrilateral continuum shell elements.

The drip shield is inclined 15 degrees with respect to the WP and the emplacement pallet to reproduce the baseline case used in the plane strain models.

The width of the Waste Package is set to 1047 mm, and to limit the number of elements in the model, the width of the shell plate is set to 38.1 mm. To reproduce the stiffness of the bulkhead plate, the modulus of elasticity of these elements is increased by the ratio of the equivalent width if the Ti-7 plate (DS report) to the selected dimension (r = 230 mm / 38.1 mm).

03-03-06

Boundary Conditions

Loads. Two base loading conditions are used: (1) pressure of 300 kPa applied normal to the DS surface, and (2) vertical forces equivalent to a projected pressure of 300 kPa. These loads are monotonically increased up to a factor of four.

Kinematic Constraints. The DS, WP, and pallet components are constrained along the line of symmetry in the y-axis direction to prevent the displacements in the x-direction (horizontal transverse direction, **Figure 3a**).

The displacement in the vertical direction (y-axis) is constrained by 4 spring elements of a relatively small stiffness on both the outer and inner shell to prevent rigid body modes. The end nodes of the outer and inner shells are constrained from the displacement in the x-direction (longitudinal).

Regarding the pallet, each node of the bottom surface is constrained from displacement in the x- and y-direction. Also, the end nodes of the pallet are constrained from displacement in z-axis direction.

Two types of constraints are used for the DS. In both cases, the displacement in the y-direction is constrained by 4 spring elements of a relatively small stiffness to prevent numerical rigid body modes. Also, the side surfaces of the bulkhead flanges and stiffeners are constrained from the displacement in z-direction to represent symmetry. In some cases, however, the DS ends are constrained in the horizontal transverse direction (x-axis), whereas in the other case the DS ends are free in all directions (**Figure 4a**).

A friction coefficient of 0.4 is used to model frictional surface interaction between the DS and WP OS, and between the WP OS and the pallet.

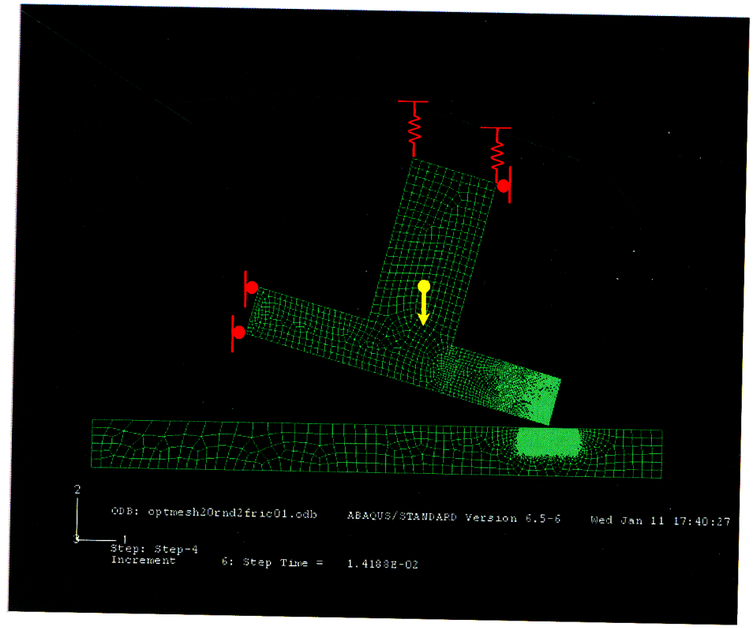

Figure 2c

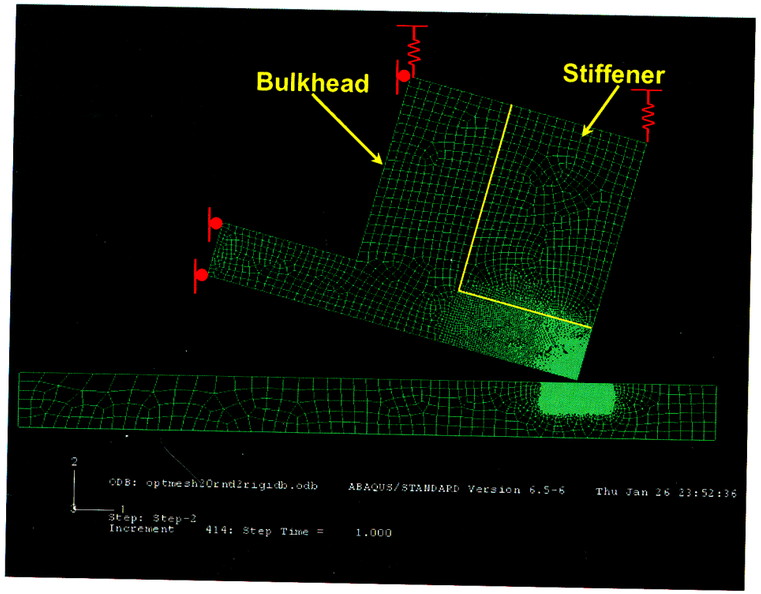

Figure 2d

03-03-06

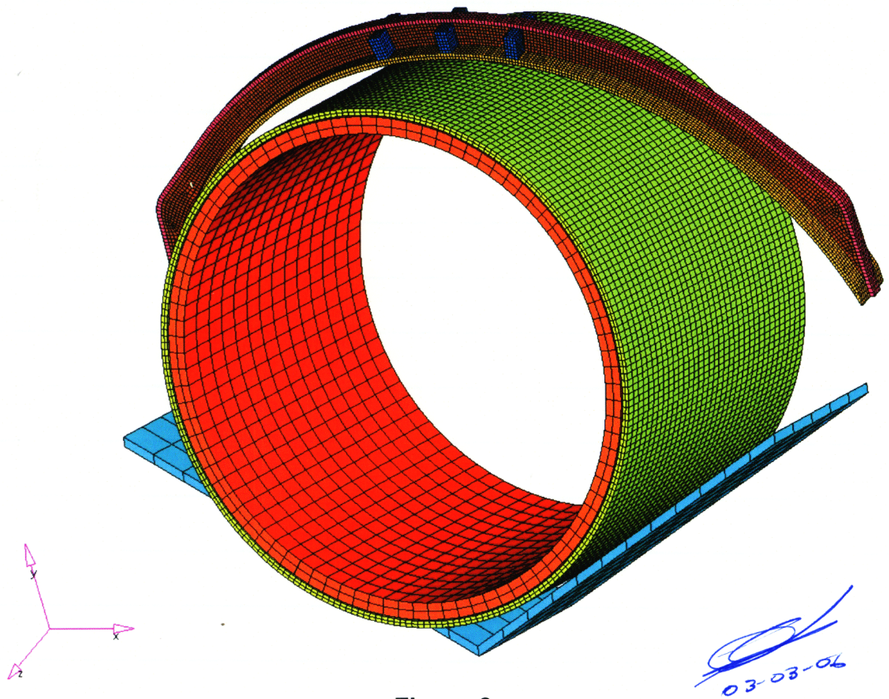

03-03-06

Figure 3a

03-03-06

Figure 4a DS Ends Constrained in the Horizontal Direction

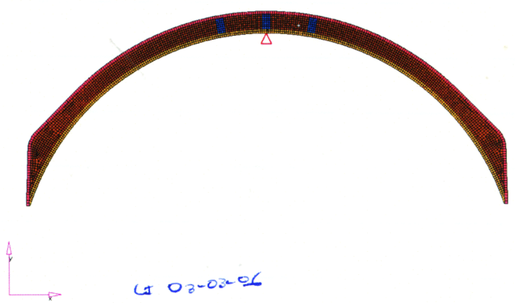

03-03-06

03-03-06

Figure 4b Free DS Ends

ANALYTICAL WP-FAILURE MODE

The FEMs of the first stage consider the reaching of the ultimate tensile strength (UTS) as the analytical failure mode.

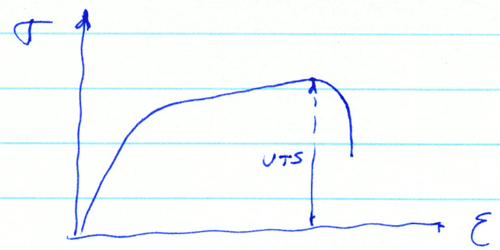

At the time the draft was sent to NRC (Jan 31, 06), the stress-strain curves requested by CNWRA to Westmoreland labs were not ready. Then, Alloy-22 material properties (LL 03/06) were obtained from the ASME code. The results are currently being updated after receiving the experimental results.

The analytical FEMs of this stage do not include deteriorating models to account for softening of the stress-strain relationship. These models cannot capture the structural performance after the UTS point is surpassed. In addition, (LL. 03/06) The approach is conservative because Failure is assumed as soon as the first Alloy 22- element reaches the UTS. See a typical displacement field in the next page, which is associated to failure (LL 03/06)

In this stage, the maximum acceptable strain is derived from an eng. strain $\epsilon_{ultimate} = 0.45$, which is equivalent to a true strain of:

$$\varepsilon_u = \ln(1+\epsilon) = 0.37.$$

Then, the strain at UTS is assumed to occur at 90% of the ultimate strain: $\varepsilon_{Failure} = 0.9\,\varepsilon_u = 0.33$

Hardening Plastic WP and Stiffener (0.25 mm radius) **15°**

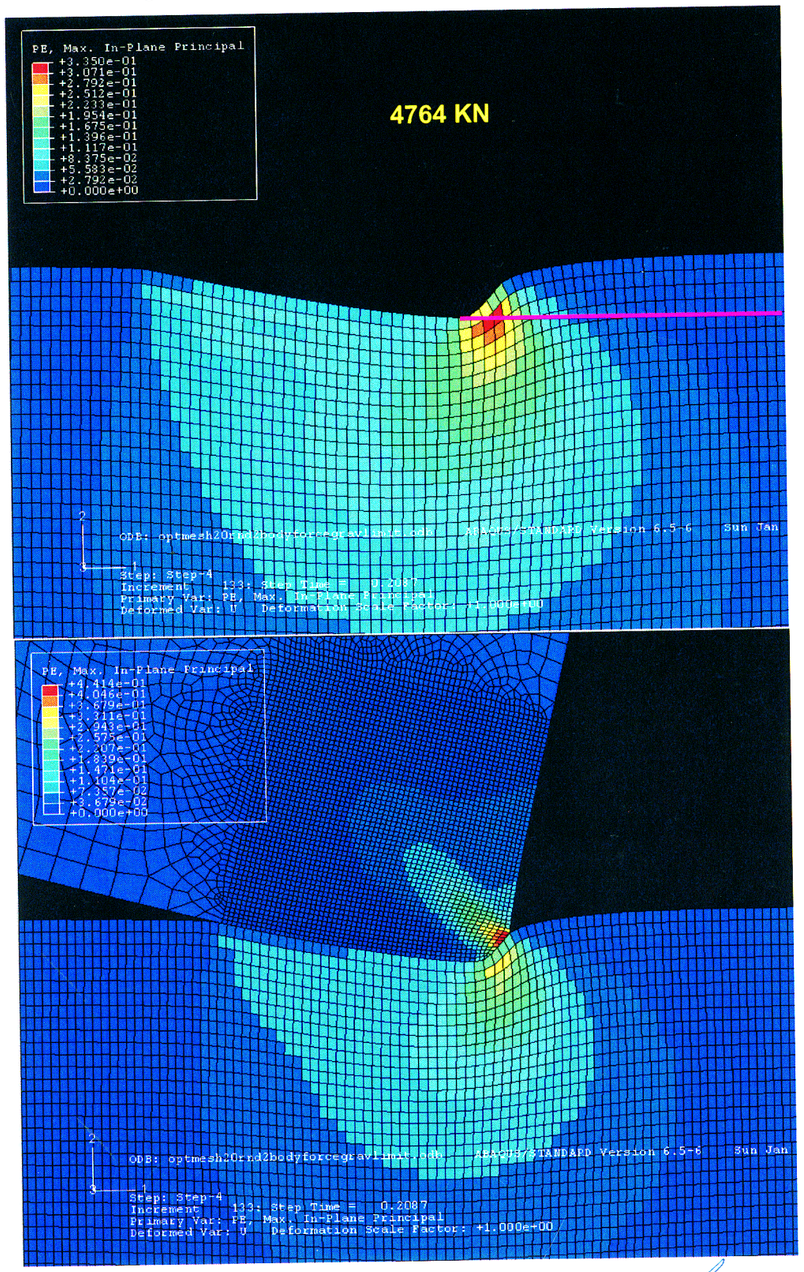

Figure 6

SENSITIVITY STUDY, CONTACT ANGLE

The effect of the contact angle WP OS capacity is obtained from a sensitivity study of plane strain models with contact angles of 0, 5, 10, 15, 20, 25, 30, 35, 40, and 45 degrees.

The curve of **Figure 9** shows the variation of the ultimate loads applied to the DS stiffener with respect to contact angle between components. The variation of the contact angle has a large effect on the maximum force that can be applied when the contact angle is smaller than about 10-15 degrees. For larger contact angles the WP OS capacity monotonically increases, but the variation is relatively small because for angles larger than about 15 degrees, the nonlinearities of the DS edge cause the contact angle to have a secondary effect. **Figure 9** also presents the WP load at failure for models with bulkhead and a contact angle of 15 degrees. The WP failure load for bulkhead cross sections with stiffeners should be comparable to that of the models with stiffeners for all contact angles, except for the zero degree contact angle case.

Figure 10a presents the variation of the contact width of the mechanical interaction with respect to the contact angle of the DS component. As observed, the increase in the contact angle does not result in a smaller contact width because the penetration of the DS component is larger, as well as the deformation of the DS edge.

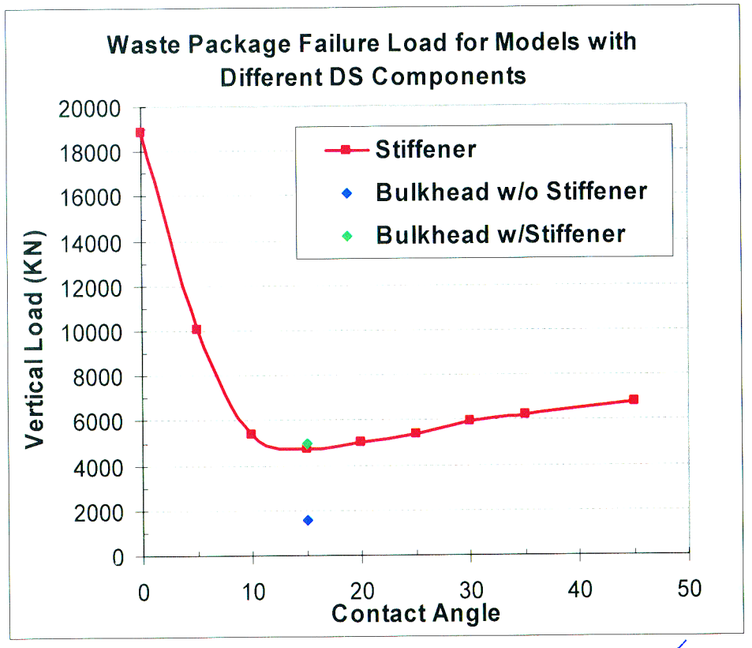

Figure 9

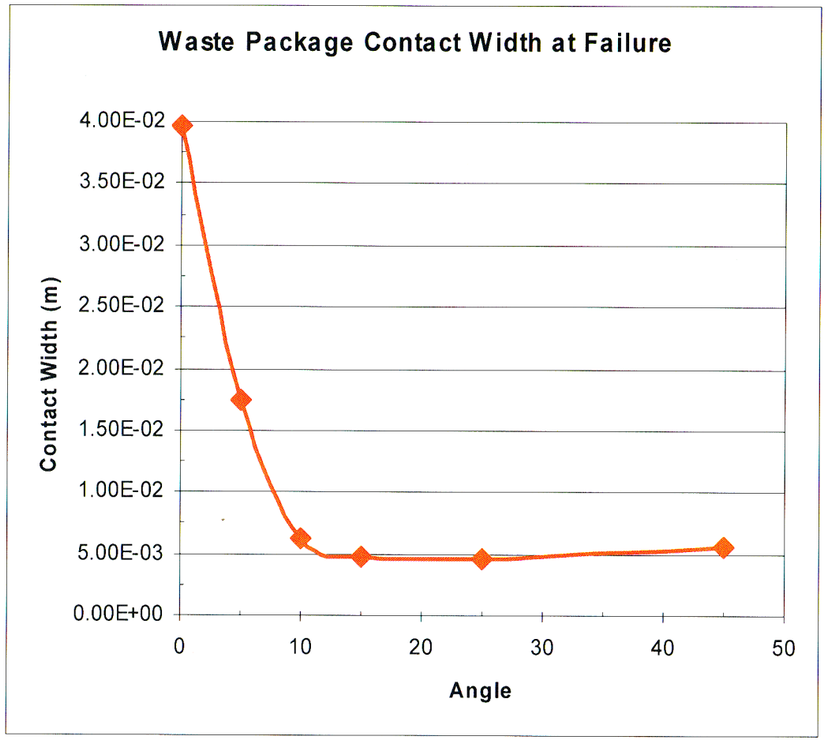

Figure 10a

03-06-06

Contact Length

The plane strain models provide the loads per unit length at which the WP OS reaches failure. To convert the loads per unit length into pressure, the contact length between the DS components and the OS needs to be obtained. The contact length increases as more load is applied on top of the DS. One of the objectives of the 3-D FEMs in ABAQUS is to determine the contact length between the DS component and the WP OS. This parameter is used to obtain an equivalent pressure from the plane strain model. Keep in mind that the data obtained from the 3-D model is for symmetric cases and for special conditions that may drastically change for different DS collapse conditions. For instance, the DS component may transfer the loads in asymmetric configurations favoring the contact length on one side of the WP OS. Also, the DS crown could severely deform previous to mechanical interaction and concentrate the forces on relatively small areas.

The results for several 3-D FEMs corroborate that the contact length is modified as the load level increases. According to the FEM results, the contact length for the pressure is approximately 500 mm under the expected loading conditions.

The contact length is used to convert the force per unit length to WP vertical pressure capacity. The following equation can be used for this conversion,

$$P_{v,WPcap} = \frac{F_{unit}}{A_{trib}} \frac{L_{cont}}{L_{unit}}$$

where F_{unit} is the force per unit length, A_{trib} is the tributary area to the DS bulkhead or stiffener (i.e., the area of DS crown that transfer loads throughout the evaluated DS component). The numerator of the non-dimensional term L_{cont} / L_{unit} is the contact length, whereas the denominator is unity.

The tributary area for bulkhead components is approximately 2.5 m^2, considering that the distance between bulkheads is 1.047 m. and that the projected width of the DS crown is about 2.5 m. These assumptions imply that the DS columns are completely unable to transfer axial loads to the DS columns once structural instability is reached due to plastic buckling of the DS columns. The DS walls, however, will be constrained by the pallet, WP, and surrounding rubble, and it is likely that the DS columns will be able to transfer a certain percentage of load, even under a DS collapsed configuration. As a result, the tributary area for the bulkhead may be smaller.

03-06-06

Tangential Loads

The baseline case for the plane strain models considers a force applied normal to the Alloy-22 plate surface. This condition may represent the mechanical interaction at the top of the WP OS, where the tangent to the cylindrical surface is initially horizontal, whereas the load transferred by the DS is due to gravity. However, if the loads are applied in other regions of the OS, the transferred loads are not perpendicular to the tangent of the OS. Several analyses were performed to evaluate this effect by modifying the tangential to normal load ratio of the system. **Figure 10c** presents the loads per unit length at the onset of WP OS failure for tangential to normal load ratios of 0, 0.25, 0.50, and 1.00, acting on a model with a contact angle of 15 degrees. **Figure 10d** shows the same information normalized by the baseline case (tangential to normal load ratio = 0). As observed, the inclusion of the tangential component improves the WP OS capacity because the contact area tends to increase.

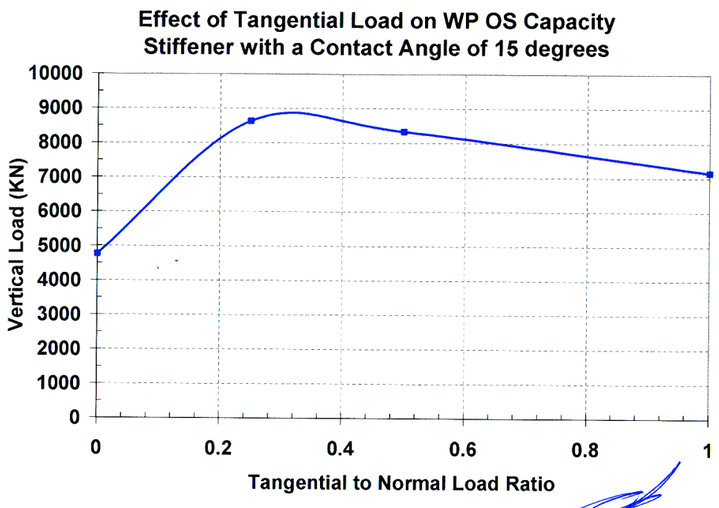

Figure 10c

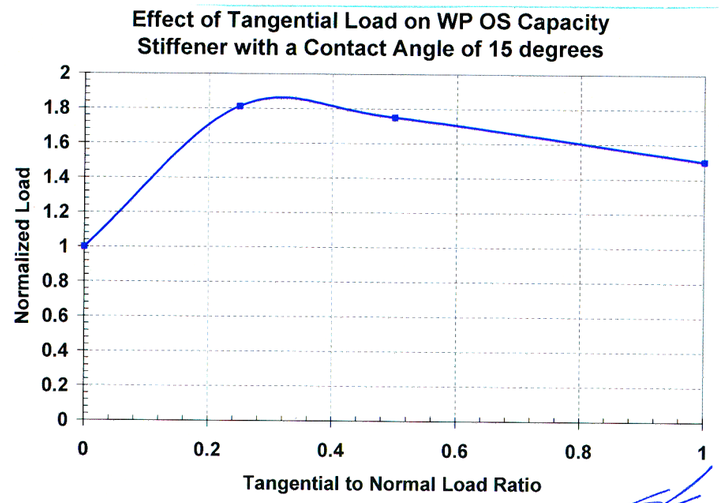

Figure 10d

Alloy-22 Plate Thickness

The Alloy-22 plate may be thinner after several hundred thousand years due to generalized corrosion. This section evaluates the variation of the capacity of the WP OS when the plate thickness is reduced. Note that it is assumed that the rate of generalized corrosion for Ti-24 is similar to that of Alloy-22. If the DS component degrades much faster than the WP OS, the sharp edges may have disappeared before the thinning of the Alloy-22 plate is large enough to decrease the ultimate load of the WP.

Figure 11 shows the decrease in the maximum load that can be applied to the WP previous to failure due to thinning of the OS plate. These analyses were performed for a contact angle of 15 degrees, which corresponds to the baseline case. The loss of WP capacity is due to a smaller number of elements capable of redistributing the stresses induced by the DS component.

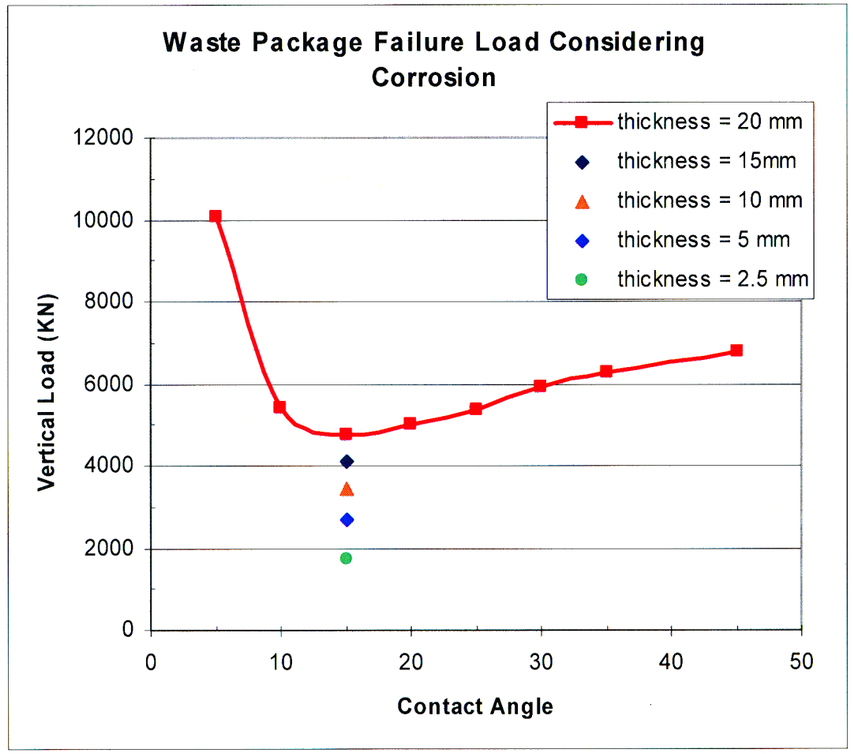

Figure 11

Thermal Effects

The engineered barriers temperature may present large variations during the postclosure period (Manepally et al). The temperature at the WP increases significantly at the beginning of the postclosure period because of the heat resulting from the emplaced waste. The temperature depends on several parameters including the potential for rockfall rubble and the time of degradation of the drift. The material mechanical properties used in the analyses of this study consider a temperature of 150 C. According to the DOE, this temperature is not exceeded during 98.5% of the repository time (considering a post-closure period of 10,000 years) when the drift remains in place. However, according to Manepally et al, if the drift degrades during the first couple hundred years, the temperature increases to about 250 C (**Figure 12**). The upper limit occurs when the drift degrades almost immediately closure of the tunnels. This extreme case presents the absolute upper boundary for the WP temperature, around 350 C. For practical purposes, however, the upper boundary can be considered as 250 C, because the stainless steel components of the ground support require several hundred years to completely degrade. Therefore, the WP temperature can be bracketed between 150 and 250 C for the first 1,000 years, which is the time in which most of the drift degradation is expected to occur.

The Alloy-22 mechanical properties, however, do not experience large modifications due to this potential temperature variation. The variation of the modulus of elasticity, yield strength, and UTS are presented in **Figure 13**. As observed, the most important decrease is in the yield strength, which is reduced about 14% when the temperature increases from 150 to 250 C. Nevertheless, the most important parameter in this evaluation, the UTS, only decreases by 6%. There is no available data regarding the strain at the UTS of Alloy-22 for different temperatures, but it is expected to be similar or larger than that at 150 C (this assumption will be corroborated based on the stress-strain experimental tests that are currently being performed). Therefore, the variation of the WP OS capacity is not evaluated for different temperatures because 250 C is a practical upper limit that may be reached under extreme circumstances, and because the mechanical properties do not decrease significantly from 150 to 250 C.

Under strong seismic events the WP temperature probably will be much lower than 150 C because these events may occur after several thousand years. According to **Figure 12**, the WP temperature may be around 50 C or lower. Nevertheless, the abstractions are not modified because the gain in UTS is very small due to this decrease in temperature (**Figure 13**), and because the material properties information does not account for exposure to higher temperatures during hundreds or thousands of years.

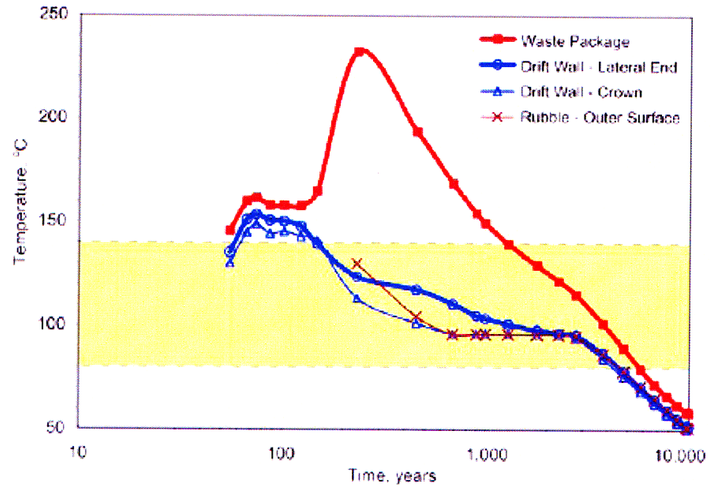

Figure 12

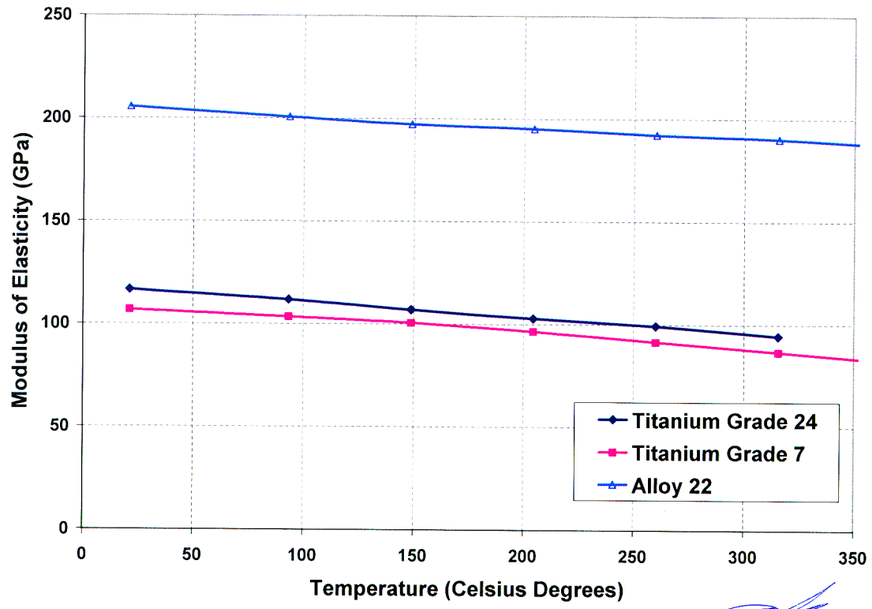

Figure 13a

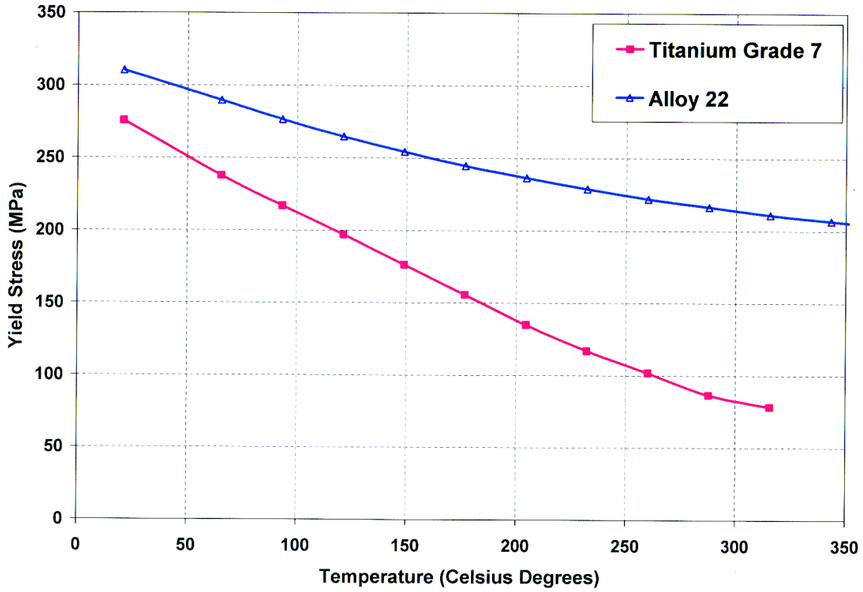

Figure 13b

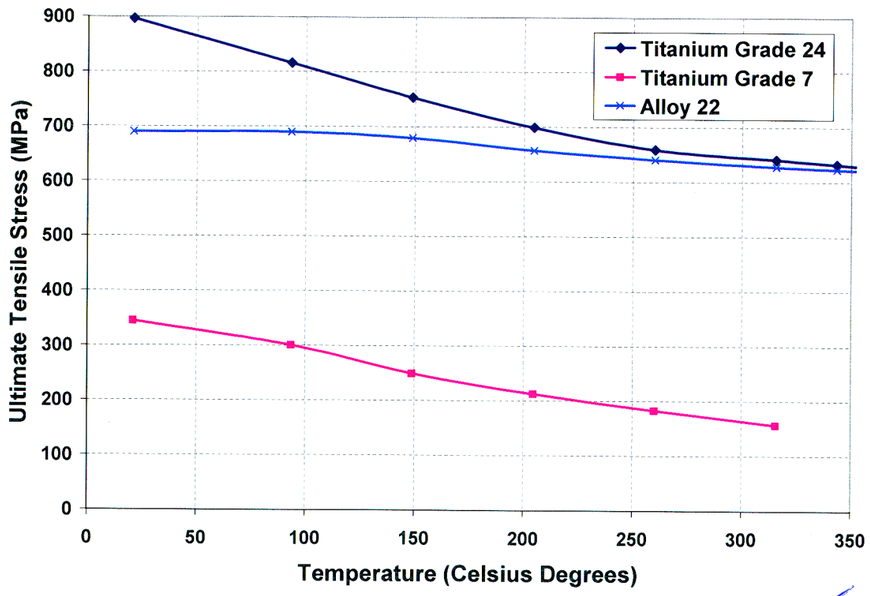

Figure 13c

03-06-06

ABSTRACTIONS DRIP SHIELD

Vertical Load (Demands)

The current MECHFAIL version computes the vertical pressure by correlating a random bulking value to the vertical pressure. The vertical pressure is estimated based on an analytical curve derived from an elliptical drift degradation geometry. The bulking factor is randomly selected by assuming a uniform distribution with lower and upper bulking factors of 1.15 and 1.25, respectively.

The updated MECHFAIL abstraction will use essentially the same approach but several modifications are introduced based on NRC/CNWRA staff judgement. First, the average vertical pressure will be delimited by the Piping and Terzaghi failure mechanisms, as suggested in the Drift Degradation Analysis report (see **Figure 14**, and DOE ...). Once the bulking factor is estimated, a weighted average will be used to select the analytical solution to be used. The Piping drift degradation geometry will be selected for 75% of the realizations, whereas the Terzaghi failure mechanism for 25% of the realizations.

The NRC/CNWRA staff also decided that the limits for bulking factors should be between 1.15 and 1.25. To adapt these criterion to the probabilistic framework, a beta distribution was proposed that includes 83% of the probability density area between bulking factor values of 1.15 and 1.25. **Figure 15** presents the probability density (pdf) and cumulative density functions (cdf) for this condition.

The general formula for the probability density function of the beta distribution is

$$f(x) = \frac{(x-a)^{p-1}(b-x)^{q-1}}{B(p,q)(b-a)^{p+q-1}}, \quad a \le x \le b;\ p,q > 0$$

03-07-06

where *p* and *q* are the shape parameters, *a* and *b* are the lower and upper bounds, respectively, of the distribution, and *B*(*p*,*q*) is the beta function. The beta function has the formula

$$B(\alpha,\beta) = \int_0^1 t^{\alpha-1}(1-t)^{\beta-1}dt$$

The case where a = 0 and b = 1 is called the standard beta distribution. The equation for the standard beta distribution is

$$f(x) = \frac{x^{p-1}(1-x)^{q-1}}{B(p,q)}, \quad 0 \le x \le 1;\ p,q > 0$$

For the distribution of the bulking factor a standard beta distribution [0,1] + 1 (i.e, a standard distribution shifted one unit) is used. The mean, μ = 0.2, and the standard deviation, σ = 0.037. Using these parameters, the following probabilities are obtained for different intervals.

P[BF < 1.1] = 0.08 %
P[BF < 1.15] = 8 %
P[BF < 1.25] = 90.6 %
P[1.15 < BF < 1.25] = 82.5 %
P[BF < 1.35] = 100 %

03-07-06